Eng. Sci., 2020, 10, 68–77

Engineered Science

DOI: https://dx.doi.org/10.30919/es8d906

Combining Silk Sericin and Surface Micropatterns in Bacterial Cellulose Dressings to Control Fibrosis and Enhance Wound Healing

Biaou O. Ode Boni, Lallepak Lamboni,* Bianza M. Bakadia, Saied A. Hussein, and Guang Yang*

Abstract

Bacterial cellulose (BC) is an advantageous wound healing matrix and widely utilized in dressings thanks to its interesting physical properties. Lacking bioactivity, BC has been subject to modifications for improving its biological properties. It has been modified with silk sericin (SS) mainly for its antioxidant and mitogenic effects, yielding enhanced wound healing abilities. Besides, patterned BC exhibited anti-scar behavior, inhibiting the growth of skin fibroblasts. Incorporating surface microgrooves together with SS in BC, the current study proposes dressings that would improve healing, reduce healing time, and still achieve reduced fibrosis, by controlling collagen deposition and inducing profitable microgroove-oriented architecture. *In vitro* experiments demonstrated an enhanced proliferation of both fibroblast and epithelial cells with alignment on the microstructured composite samples relative to the unmodified controls. Compared to the unmodified control where collagen synthesis was rapid and reached the peak value in a relatively short time, on the microstructured surface a progressive and more contained profile was observed. Thus, the structured composite dressings would accelerate healing due to an improved cell growth, while preventing the anarchic deposition of collagen responsible for fibrosis and scar formation through cell orientation.

Keywords: Microstructured bacterial cellulose; Silk sericin; Wound dressing; Collagen deposition; Fibrosis.
Received date: 26 March 2020; Accepted date: 29 April 2020
Article type: Research article

1. Introduction

As one of the most vital organs, the skin constitutes the main protective barrier of the body against microbes and other harmful elements present in the environment; it also preserves the balance of electrolytes and water while regulating body temperature.[1] However, it constantly incurs high risks of damage due to repeated exposures to potentially harmful assaults, which disrupt the body's homeostasis. While altered skin tissue generally initiates a complex wound healing cascade to repair itself, acute but major trauma such as burns, or chronic wounds and surgery-related sequels often involve extensive debilitating skin losses that degrade the quality of life, with the potential of causing death.[2] To optimize healing, wound dressings are thus utilized that possess antimicrobial properties to prevent infection, and bioactive abilities that enable interactions with wound cellular actors to activate healing. Moreover, the ideal wound dressing should keep a clean wound bed by absorbing exudates while enabling gas exchange and maintaining a moist environment to limit dryness and pain.[3]

Bacterial cellulose (BC) has a nanofibrous and porous structure, which provides a good water retention ability and enables oxygen permeability.[4] It is biocompatible and presents high tensile strength and flexibility[5] with an overall great potential for wound healing,[6] though lacking antimicrobial and bioactive properties.[7] To overcome the latter and improve BC as a wound dressing, studies have been conducted on the combination of BC with other materials.[8,9]

Commonly extracted from silk cocoons, silk sericin (SS) is a protein with antioxidant, anti-tyrosinase, antimicrobial and moisturizing properties, all of which are beneficial to skin repair.[10] Interestingly, studies have shown that SS promotes

National Engineering Research Center for Nano-Medicine, Department of Biomedical Engineering, College of Life Science and Technology, Huazhong University of Science and Technology, 1037 Luoyu Road, Wuhan, 430074, P.R. China
**: Email: lallepak@yahoo.fr(L. Lamboni); yang_sunny@yahoo.com(G. Yang)*

the proliferation of fibroblasts and the production of collagen, indicating an active involvement in wound healing.[11-13] Moreover, it has been reported that SS increases the expression of vascular endothelial growth factor and promotes wound angiogenesis,[14] favoring new tissue formation. However, due to its inadequate mechanical properties,[15] SS is limited as material, often requiring reinforcement by other polymers for the fabrication of stable and sustainable biomaterials.

To exploit the advantages of both BC and SS, in a previous study, we combined these materials for wound dressing applications. The BC-SS composites showed promise for wound healing by promoting the proliferation of fibroblasts while supporting the growth of keratinocytes.[16] Meanwhile, a recent study by Jin *et al*. reported that designing the BC surface to present microgrooves inhibits the proliferation of L929 cells and reduces the abnormal deposition of collagen and scar thickness.[17] Indeed, material surface topography controls both cell behavior and tissue function,[18,19] and it has been one of the objectives of recent tissue engineering to restore tissue function by exploiting biomimicking devices. Hence, emulating the structure and architecture of the natural extracellular matrix (ECM) in a tissue-specific manner to promote tissue regeneration has been the center of numerous studies.[20-22] For wound healing applications, the target is not only achieving a rapid wound closure to avoid infection, but also instigating an ECM formation favorable to reducing fibrosis and scar formation. Thus, Lu *et al*.[23] recently reported silk fibroin-based scaffolds of aligned fibers that improved the overall wound healing with enhanced cell migration and vascularization as compared to non-aligned scaffolds, and effectively replicated collagen architecture found in non-wounded tissue in the rat's healed skin. Another study exploited the meshed structure of BC membrane, upon which crossed grooves structures had been imprinted using photolithography induce native tissue-like collagen structure in the rat skin wounds.[24] When stripe structures were formed on the BC membrane during biosynthesis, inflammation, which is also a hallmark of scars, was considerably reduced in animal wound healing, leading to reduced scar sizes.[17, 25] Hence, we aimed in this study to capitalize on both topographical cues and biochemical composition to obtain a biomaterial with improved biomimicry for enhanced tissue regenerations. We imparted microgroove structures to BC using poly(dimethyl siloxane) (PDMS) templates, and then functionalized the materials with SS to alleviate the cell growth inhibition reported by Jin *et al*.[17] with the aim of not only inducing unwounded-like collagen architecture but further accelerating wound healing. *In vitro* studies were carried out to explore the effects of the proposed dressing samples on the behavior of fibroblast and epithelial cells, main cellular actors of skin wound healing. Moreover, the collagen production from fibroblasts was evaluated to verify the assumption of the current study. Additionally, the physico-chemical characteristics of the samples were also herein included.

2. Materials and methods

2.1 Materials and chemicals

In the current study, following reagents were used: *Acetobacter xylinum* (ATCC53582); yeast extract and peptone (Oxoid Ltd, UK); *Bombyx mori* cocoons (Ningbo Industrial Co., Ltd); microfilter (0.2 μm pore size, Millex GP filter); NIH-3T3 (mouse embryonic fibroblast cell line) and HaCaT (human skin keratinocytes) cell lines (China Infrastructure of Cell Line Resources); Dulbecco's modified eagle medium (DMEM, Hyclone); phosphate buffer saline (PBS, Hyclone); fetal bovine serum (FBS) and penicillin-streptomycin (Gibco); Cell counting kit-8 (CCK8, Dojindo); BCA protein assay kit (Solarbio, Life Technologies); total collagen assay kit (Quickzyme Biosciences); fluorescein isothiocyanate labeled phalloidin (FITC-Phalloidin, Yeasen); Hoechst 33342 (Invitrogen, Life Technologies). All other reagents were of chemical grade.

2.2 Preparation of bacterial cellulose

Hestrin & Schramm medium for the culture of *Acetobacter xylinum* was prepared as described previously.[16] To produce the control BC with randomly organized fibers (rBC, 1-2 mm thick), a suspension of the bacteria was seeded in an autoclave-sterilized medium, the flat surface of PDMS was deposited in contact of media, and incubated in static conditions at 30°C for 5-7 days. To obtain the microstructured BC (mBC), before culture as above, PDMS templates presenting microgrooves were deposited on the surface of the medium immediately after bacteria inoculation, with the micropatterns facing the liquid media so that to mold the BC fibers upon excretion by the bacteria (Fig. 1).[26] Based on previous studies, the templates in this study were designed with microgrooves of 10 μm width.[17,27] BC was cleaned as previously described and autoclaved before storing at 4 °C until use.[16]

2.3 Extraction of silk sericin and preparation of BC-SS composites

SS extraction from *Bombyx mori* cocoons and the preparation of SS solutions as well as the composites were performed according to the reported procedures.[16] Briefly, after obtaining the SS solutions, BC was immersed in the latter and kept at room temperature for 24 h to obtain the composite, which was thereafter rinsed in phosphate-buffered saline (PBS) to remove excess SS (Fig. 1). Different SS concentrations were prepared (i.e., 1%, 2%, and 3%) to fabricate respective composites, namely BC-SS1, BC-SS2, and BC-SS3. For biological studies, SS solutions were microfilter-sterilized before composite preparation.

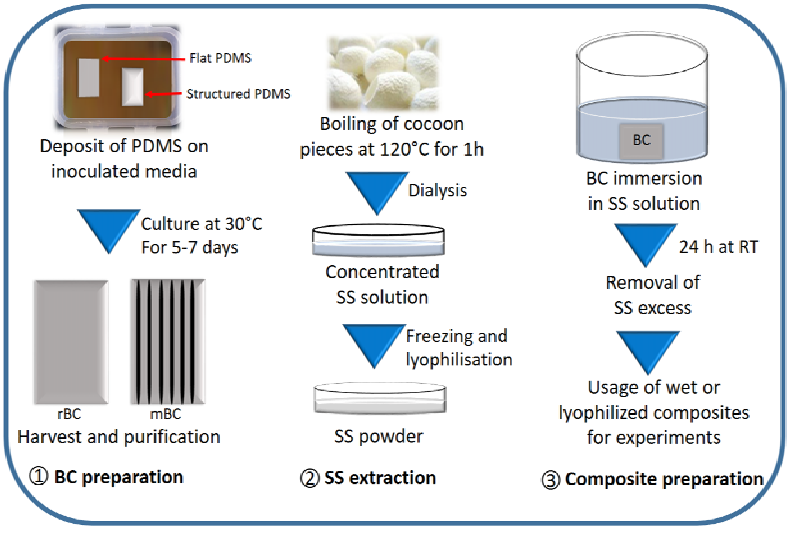

Fig. 1. Preparation of rBC, mBC, SS powder, and BC-SS composites. To generate random BC (rBC), flat surface of poly (dimethyl siloxane) (PDMS) was deposited on the interface of bacteria inoculated media while to obtain microstructured BC (mBC), PDMS templates presenting microgrooves were deposited on the surface of the medium with the micropatterns facing the liquid media so that to mold the BC upon excretion by bacteria. RT = room temperature.

2.4 Physico-chemical characterization of the samples

For characterization tests, samples were prepared and freeze-dried beforehand. The morphology of the BC structure and evidence of the incorporation of SS were visualized under a scanning electron microscope (Nano SEM 450) on platinum coated samples. To study the chemical interactions between BC and SS, 64 scans were accumulated at a 2 cm^{-1} resolution in the range 4000-400 cm^{-1} by Fourier transform infrared (FTIR, vertex 70, Bruker) spectroscopy. Samples' crystallinity was assessed by X-ray diffraction (XRD, PA Nanalytical, EMPYREAN), by scanning the samples at 2-theta diffraction angles from 10° to 70°.

Mechanical properties were measured by the tensile testing (Shenzhen Suns Technology Stock Co, Ltd). All samples (~2 mm thickness) were wet and cut in rectangular shape (50 mm×8 mm) following the direction of the microgrooves for mBC. Moreover, the microgrooves were arranged in the direction of the stretching force during testing. The crosshead speed of *** mm/min was used for this test. For each sample, the test was performed on three specimens.

2.5 Swelling test

To determine the ability of different substrates in absorbing water, gravimetric method was used.[27] Freeze-dried samples (1.4×1.4 cm^2) were weighed (*Wi*) before immersion in distilled water and incubation at 37 °C for different time-points (i.e., 1, 6, 12, 24, 48, and 72 h). At each time interval, samples were removed from the water, and weighed again to determine the final swollen weight (*Wf*) after the removal of excess water on absorbent paper. Three replicates were used at each time-point. The swelling ratio was calculated using formula (1):

$$\text{Swelling ratio } (\%) = \frac{(\text{wf} - \text{wi})}{\text{wi}} \times 100 \qquad (1)$$

2.6 Determination of SS release profile

Lyophilized composites (1.4×1.4 cm^2) were used. Each of these was immersed in PBS solution (identical volume for all samples) and incubated at 37 °C under shaking. Supernatants were collected at 0, 1, 15, 30 min and 1, 12, 24, 48 and 72 h after incubation to measure the amount of SS released by each composite. Three replicates were used for each time-point. The cumulative amount of SS released by each composite was assayed by colorimetry, using the BCA protein assay kit. Absorbance was measured in a microplate reader (Multiskan Go, Thermo scientific) at 562 nm.

2.7 Biocompatibility tests

To evaluate the ability of the materials to support cell growth and skin regeneration, the viability of NIH-3T3 (mouse embryonic fibroblast cell line) and HaCaT (human skin keratinocytes) cells on these substrates was tested. Before and during the tests, the cells were cultured at 37 °C and 5% CO_2 humidified atmosphere in DMEM supplemented at 10% with FBS and 1% penicillin/streptomycin. Subculture was performed at a cell confluence of 80 -90% and after 4 to 7 passages, the cells were seeded on the samples.

Two types of *in vitro* biocompatibility tests were performed, assaying cell viability with CCK8. Namely, both the cytotoxicity of samples' extracts and the biocompatibility of the substrates by direct contact with cells were investigated. To obtain the extracts, the samples (1.4×1.4 cm^2) were immersed in 1 mL of the cell culture media for 24 h at 37 °C; after which extracts were collected and stored at 4 °C until use (ISO 10993-5:2009 (E)). After 24-hour culture of 10^4 cells (per well) in 96 well plates, the media was replaced with extracts of respective samples. The viability test was then performed 1, and 3 days later by replacing the extracts

with fresh media containing 10% (v/v) of the CCK8 reagent. Following 1-hour incubation in the dark, the absorbance was measured on supernatant aliquots at 450 nm in a microplate reader (Multiskan Go, Thermo scientific). Samples were tested in triplicates.

For the direct contact test, the samples were laid at the bottom of 24-well plates ensuring by visual control under microscope that the top structured surface of the mBC samples was positioned upwards. Cells (6×10^4 per sample) were seeded on the top surface of each membrane sample. After 1, 3 and 5 days culture, the viability test was then performed by CCK8 test as described above. Samples were tested in triplicates.

2.8 Confocal microscopy

To observe cell morphology and organization, actin filaments and cell nuclei were stained by FITC-Phalloidin and Hoechst 33342, respectively, and visualized by confocal microscopy (Olympus fluoview FV100). Cells (10^4 per membrane) were grown for 3 and 7 days, respectively, in 96 well plates. For cell staining, manufacturer's instructions were followed. Samples were kept in PBS at 4 °C for 24 hours before mounting for confocal microscopy.

2.9 Determination of collagen production

To measure collagen production, 6×10^4 fibroblast cells were seeded per sample in 24 well plates as described above. Cell culture medium was replaced every 72 h, with the old one being collected in eppendorf tubes and stored at -20 °C until use. After 5 and 7 days culture, respectively, collected supernatants were mixed right before the test, yielding a cumulative concentration of the soluble collagen produced by the cells, which was measured by the total collagen assay kit. The principle of this test is to measure the total amount of hydroxyproline present in the supernatant, which represents the total amount of all types of collagen synthesized by the cells and released at the surface of supporting material samples. The test was carried out following the procedures instructed by the manufacturer.

2.10 Statistical analysis

One-way analysis of variance (ANOVA) was used with Tukey's multiple comparison to compare different experimental groups. All statistical analyses were performed with Origin Pro 8 software. The statistical significance was obtained at $P < 0.05$.

3. Results and discussion

3.1 Physico-chemical characterization

3.1.1 SEM, FTIR and XRD of samples

Scanning electron microscopy was performed to verify the morphology of different samples. In Fig. 2, rBC and mBC both present fibrous networks with interconnecting pores, which characterize the BC structure.[28] However, the top surface of mBC presents microgrooves with aligned fibers, which replicate the line structures of the PDMS templates used during sample preparation, contrary to rBC where fibers are randomly arranged throughout the structure. Interestingly, the line structures in mBC have been shown to organize and direct the cell layout in that same pattern as targeted in the current study.[19] Moreover, relative to rBC, mBC exhibits denser and more compactly packed fibers, with reduced pores, which are capable of improving the mechanical properties of BC especially its strength.[27] Images of the BC-SS composites show the incorporation of SS which appears on the surface of the BC fibers as a coating and with particle aggregates. The incorporation of SS moderately affects the porous structure of BC by filling pores although not significantly, which could affect the water absorption ability of BC. Meanwhile, the incorporation of SS does not affect the surface microstructure of the mBC. Cross-section images of BC show layers of fibers superimposed on each other and interconnected by pores, more organized in mBC than in rBC. Moreover, the bottom sides are more porous than the top, as reported.[28]

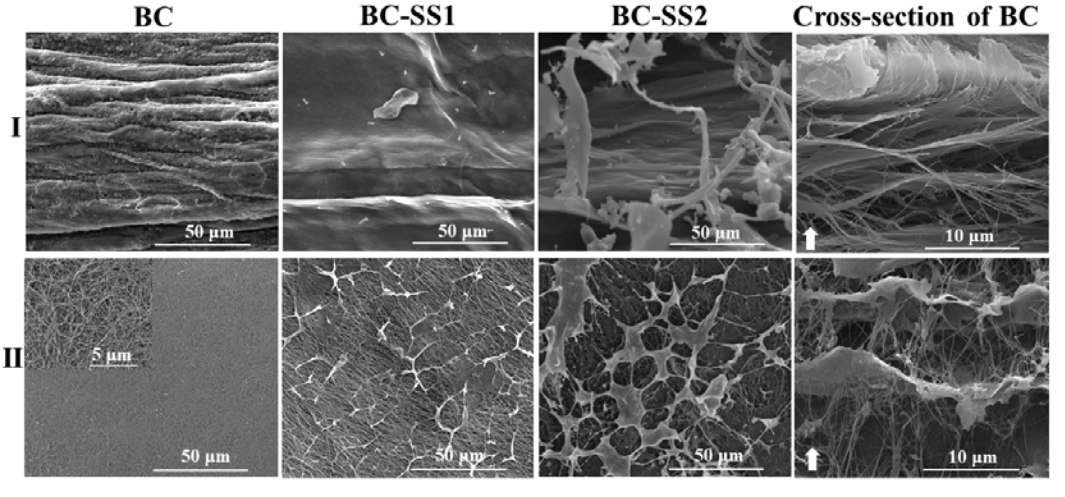

Fig. 2. SEM images. I: mBC, II: rBC. mBC displays aligned fibers with presence of microgrooves, whereas the fibers of rBC are randomly arranged. Arrows: indicate the direction from the bottom towards the top surface.

FTIR analysis was performed and different spectra are illustrated in Fig. 3a. mBC and rBC present similar spectra, with typical cellulose bands between 3200 and 3440 cm^{-1} (OH stretching, and inter- and intra- molecular hydrogen bonds stretching), at 2894 cm^{-1} (C-H stretching for alkanes and asymmetric CH_2 stretching), 1639 cm^{-1} (carbonyl groups of glucose), 1050 cm^{-1} (C-O-C stretching), and 899 cm^{-1} (β-glycosidic linkages).[29] The mBC spectra exhibits sharper hydrogen bonds stretching compared to rBC, which would make it more stable by improving its mechanical properties; moreover, hydrogen bonds have the advantage of enabling the entrapment of water molecules, beneficial for wound dressing applications. As documented,[30] the spectrum of SS presents protein characteristic bands, with peaks between 1650 and 1620 cm^{-1} (primary amides) and 1540 to 1500 cm^{-1} (secondary amides) representing random coils, and from 1270 to 1215 cm^{-1} (tertiary amides, β-sheets). Another peak centering at 3274 cm^{-1} (free hydroxyl groups and the vibration of -NH groups) is observed. For different BC-SS composites, both characteristic peaks of BC and SS were in the spectra, proving the successful incorporation of SS into BC. The decreased intensity of the peak relative to OH groups in BC-SS spectra comparatively to BC spectra, and merged the peak of the hydrogen bonds of SS (3274 cm^{-1}) with that of BC (3350 cm^{-1}) indicated the decrease of these bonds of BC, which can be explained by their engagement in hydrogen bonds with other functional groups of SS such as amides and amine groups.[16]

To confirm sample crystallinity, XRD was used, Fig. 3b. The BC exhibits crystalline peaks at 2θ=14.5° and 2θ= 22.5°, characteristic of native cellulose and corresponding to the I_α and I_β phases of cellulose crystal planes, respectively.[9] The BC spectra exhibit a third peak between 19° and 20° which corresponds to its amorphous constituent, thus confirming its semi-crystalline structure.[31] The intensity of the peak at 2θ=22.5° in mBC is higher than that in rBC, suggesting the higher crystallinity of mBC compared to rBC. SS displays a broad peak from 19° to 29° which indicates its amorphous nature.[32] The BC-SS composites show similar peaks to pure BC, with the preservation of the crystalline peaks of BC, suggesting that SS does not affect the BC's crystallinity.

3.1.2 Swelling ability

Fig. 4a illustrates the swelling ratio of the samples at different time points. The swelling ratio of mBC is higher than that of rBC during the first hour. Because of the high hydrogen bonds in mBC structure, the latter rapidly binds water molecules and becomes saturated while rBC retains more water over time by storing it in the pores. The swelling ratio of pure BC is significantly higher than that of respective BC-SS composites, and the water absorption capacity of the latter decreases with increasing the SS

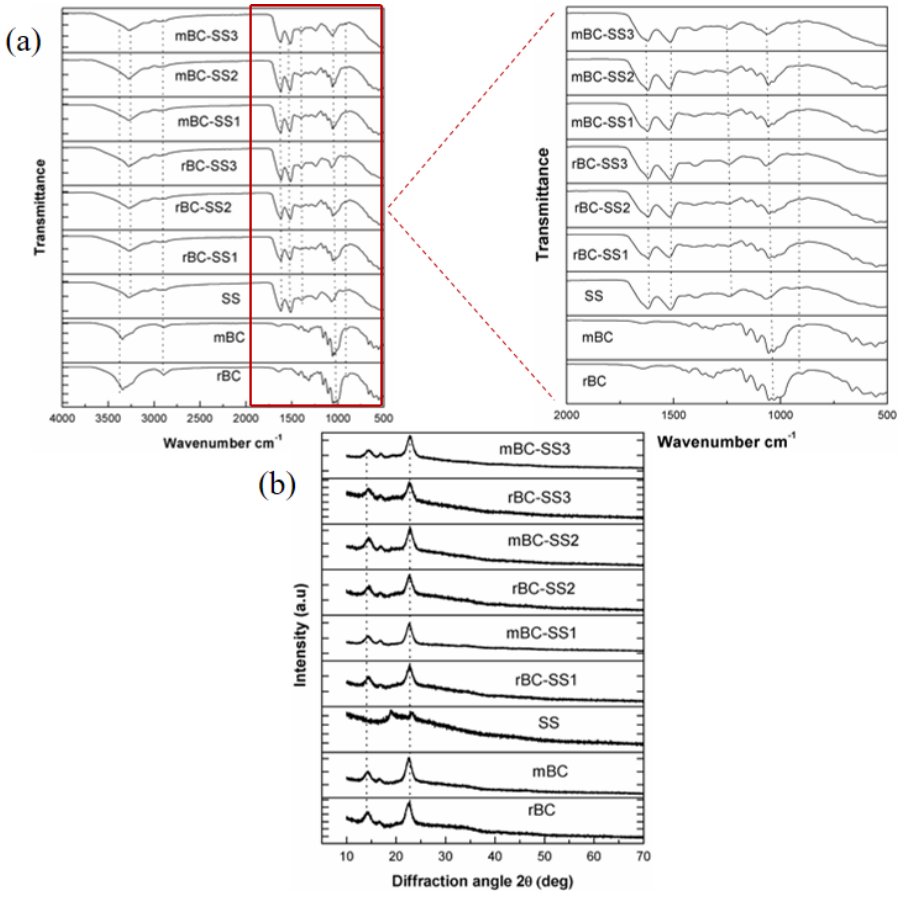

Fig. 3. Sample characterization by (a) FTIR and (b) XRD. Compared to rBC, mBC exhibits more hydrogen bonds responsible for higher crystallinities relatively to the former. These parameters decrease slightly with the incorporation of SS.

concentration. This agrees with the SEM results which show the porosity reduction in the composites due to the incorporation of SS. Moreover, after the first hour and at equilibrium, rBC-SS composites retain more water than those of mBC-SS. Nevertheless, all samples have good water retention, necessary for the removal of wound exudates.

3.1.3 *In vitro* SS release

Fig. 4b shows SS release in physiological-like conditions at different time intervals. The maximum amount of SS was released 6 h after immersion in PBS, facilitated by the non-covalent interaction between BC and SS. SS release varied with the concentration of the SS solution utilized for the composite preparation, with higher SS concentrations responsible for a higher protein release amount. rBC-SS composites released more SS than mBC-SS, due to the higher porosity of rBC which enables higher uptakes of the SS solution relative to mBC during the sample preparation. The results show the rapid release of SS within 1 h, which would be of great importance for cell growth and collagen synthesis during wound healing.

3.1.4 Mechanical stability

Tensile testing was employed to assess materials' mechanical stability. Fig. 4c&d shows the stress-strain curves and Young's moduli of the samples, respectively. The stiffness of mBC was significantly higher than that of rBC, which can be explained by the denser fiber network of the former as suggested by the SEM images. This can also be explained by the higher number of hydrogen bonds in the mBC structure which make the latter more stable. Conversely, the elongation at break of rBC was higher than that of mBC. Thus, the compact and orderly arrangement of fibers in mBC improved its mechanical strength but moderately reduced its flexibility compared to rBC.[27] In the composites, the mechanical strength was decreased compared to pure BC, due to the amorphous nature of SS which decreased the overall mechanical strength of the composite matrices.[15, 33]

3.2 Biocompatibility of the materials

To ensure their non-toxicity in wound dressing applications, the materials were tested for biocompatibility using skin cell lines including fibroblasts (NIH-3T3) responsible for the synthesis of collagen (ECM protein participating in the architecture of new tissue), and keratinocytes (HaCaT) which make up the first layer of skin (epidermis; ensures the barrier function of skin). Cell viability was measured in the presence of sample extracts on one hand (Fig. 5a-b), and following direct contact of the cells with the samples on the other (Fig. 5c-d). When extracts were applied, at day 1 the percentage of viable cells in composites' extracts was significantly higher than that of the positive control (routine culture media) and pure BC, confirming that SS which is released in the extracts improves the proliferation of fibroblast and epithelial cells. The cell growth was reduced on the 3rd day for NIH-3T3 and HaCaT respectively, due to the saturation of the allocated growth surface. Moreover, keratinocytes were more viable in the presence of rBC-SS extracts than in those from mBC-SS, in agreement with the in *vitro* SS release profile which shows that rBC-SS releases more SS than mBC-SS.

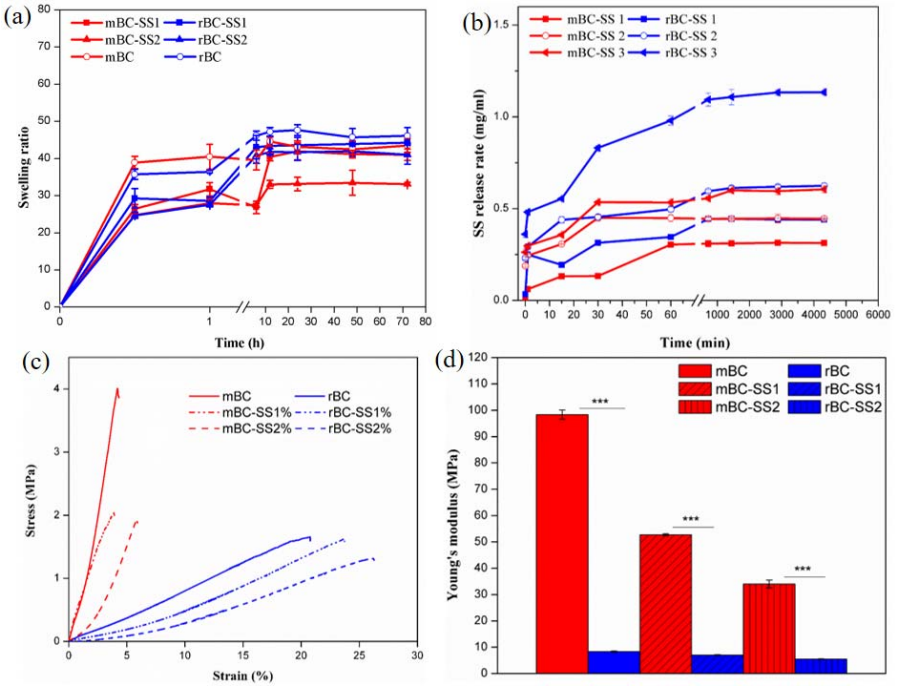

Fig. 4. Physical properties of the materials. (a) Sample swelling behavior; (b) SS release profile from the composites; (c)-(d) Mechanical properties. Because rBC is more porous, it absorbs more water than mBC; It also uptakes more SS solution during the composite preparation, leading to a higher SS release from this sample than mBC. Further, mBC displays significantly higher stiffness than rBC.

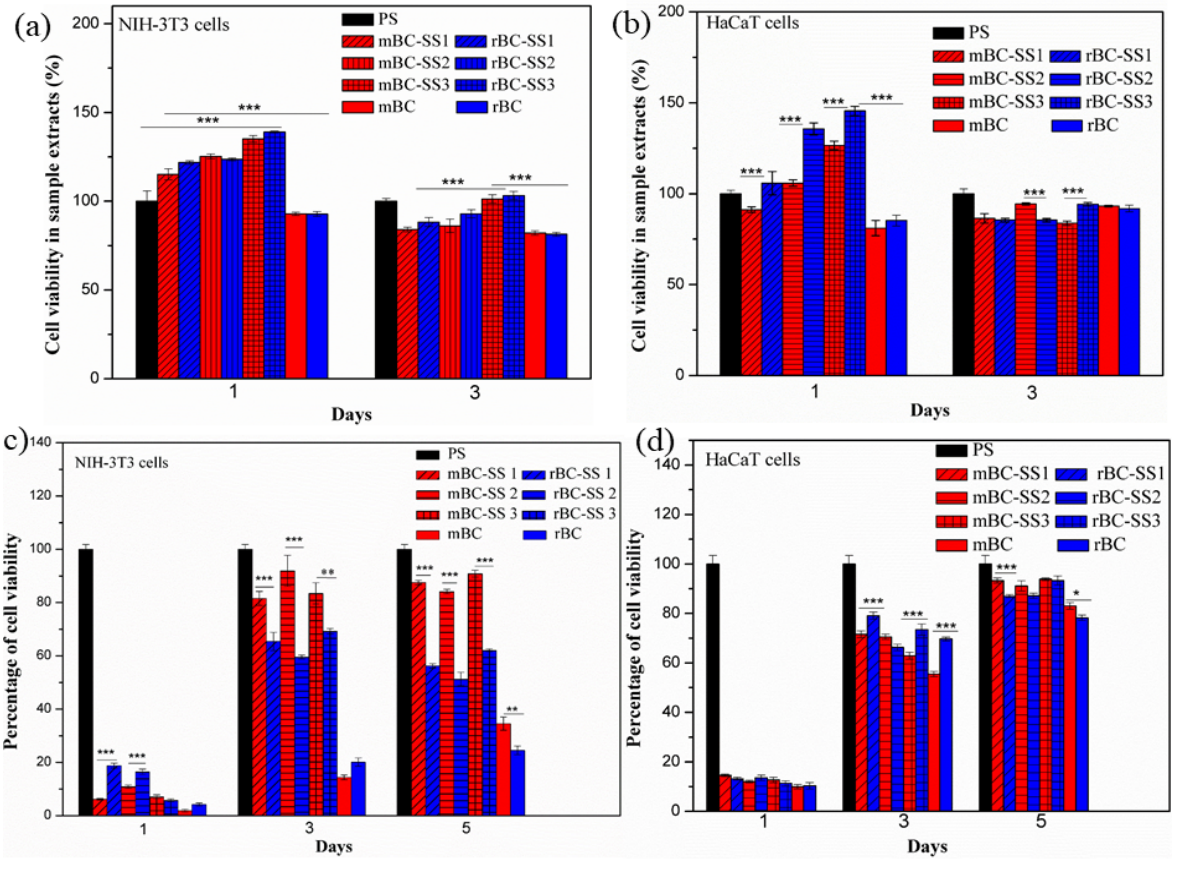

Fig. 5. *In vitro* biocompatibility of samples. (a, b) Cell viability in sample extracts, 10^4 cells per well of 96 well plates. (c, d) Cell viability on the biomaterials, 6×10^4 cells per membrane in 24 well plates. (***) $P < 0.001$; (**) $P < 0.01$; (*) $P < 0.05$. All samples demonstrate the ability to support cell attachment and growth.

To evaluate the attachment and proliferation of cells on the materials, the cells were seeded on the latter. The percentage of viable fibroblasts on mBC was low compared to those on rBC at days 1 and 3 though with no statistical difference, due to initially higher cell attachment on rBC. By contrast, after 5 days, the cell growth was significantly higher on mBC compared to rBC, indicating the progressive but higher proliferation rate of fibroblasts on mBC than on rBC, which may derive from different physical properties of the samples. Same profile was observed for keratinocytes, with statistical differences at days 3 and 5. Our result for day 5 is contrary to that reported by Jin *et al.*[17] where microgrooves of 10 μm width inhibited the proliferation of L929 even at day 5, probably due to the higher seeding cell density in our experiments which enhanced cell viability.[34] After 3 and 5 days culture, cell growth on the different samples was significantly higher than that at day 1, implying that all samples support the proliferation of both cell types. Furthermore, the viability of both cell types was significantly improved on the composites relatively to pure BC, confirming the extract test results and the bioactivity of the SS released by the composites. In fact, SS is reported to improve fibroblast and epithelial cells proliferation through its mitogenic property, while preserving cell integrity, thanks to its antioxidant ability.[11] At day 3, the fibroblast viability on BC-SS2 was higher than that on BC-SS1 and BC-SS3, suggesting an optimal SS concentration around 2%.

In physiological conditions, the proposed samples release SS that improves the proliferation of fibroblast and epithelial cells, which would improve tissue regeneration. Therefore, both rBC-SS and mBC-SS have the potential of enhancing wound healing. However, mBC appears to be the best dressing material because it is able to induce fibroblast cell alignment, ultimately controlling the anarchic deposition of collagen which could lead to the formation of fibrosis and scar.

3.3 Effects of the microstructured surface on cell behavior

Uncontrolled cell proliferation and architecture, particularly of fibroblasts, can lead to anarchic synthesis and deposition of collagen with the formation of fibrosis during wound healing.[35] Interestingly, these can be controlled by inducing cell orientation through structuring the surface of the dressing. Fig. 6 shows the confocal microscope images of the NIH-3T3 and HaCaT cells grown on the samples and stained for F-actin. At day 3, fibroblasts were more spread on the composites compared to pure BC, consistent with the cell viability results which support that cells are more viable on the composites than on pure BC. Before day 3, cells were non-spread as in previous studies, supposedly due to the

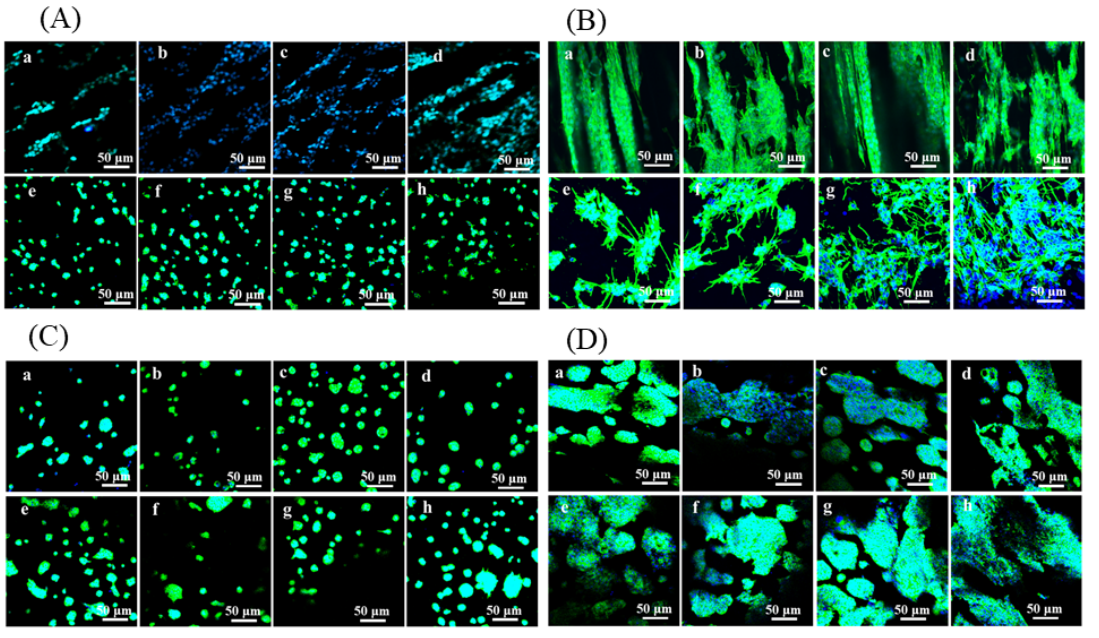

Fig. 6. Confocal images of fibroblasts (A-B) and keratinocytes (C-D) cultured onto scaffolds (10^4 cells / sample, 96 well plates) for 3 and 7 days respectively. The cells align on the microgrooves of mBC, while arranging randomly on rBC. Keratinocytes exhibit similar morphologies on mBC and rBC. Green: actin filaments; blue: nuclei. a: mBC, b: mBC-SS1, c: mBC-SS2, d: mBC-SS3, e: rBC, f: rBC-SS1, g: rBC-SS2, h: rBC-SS3.

surface tension and stiffness of BC.[36] Fibroblasts appeared to align on mBC, which was confirmed by culturing them for 7 days. At day 7, they were well aligned on mBC and mBC-SS according to the orientation of the microgrooves. By contrast, the cells on rBC and rBC-SS were aggregated and randomly distributed on the surface of the membrane. Hence, the line structures on mBC induce fibroblast cell alignment, corroborating reports that microstructure designs at the surface of biomaterials define the behavior of the cells they support, both in terms of morphology and distribution.[26] At day 3, keratinocytes were also non-spread on the samples, but were denser on the composites. At day 7, they adopted the aligned pattern on mBC, while still arranged in bulk on rBC. However, the alignment was not as well defined and uniform as for fibroblasts, probably due to the strong adhesion of the epithelial cells to each other and their round morphology. In conclusion, the microstructured surface of BC affected the architecture and distribution of the studied cells and particularly fibroblasts, which is of great importance for inducing the orderly and uniform deposition of collagen desired to prevent excessive fibrosis.

3.4 Collagen production from fibroblasts seeded on the biomaterials

Collagen is an important ECM protein, determinant of the remodeling stage of wound healing. Fig. 7 shows the level of soluble collagen released by fibroblasts grown on different samples at different times. In the presence of BC-SS composites, the amount of collagen was higher than for pure BC samples. In fact, SS contains a high level of methionine which promotes rapid fibroblast growth and collagen production.[37]

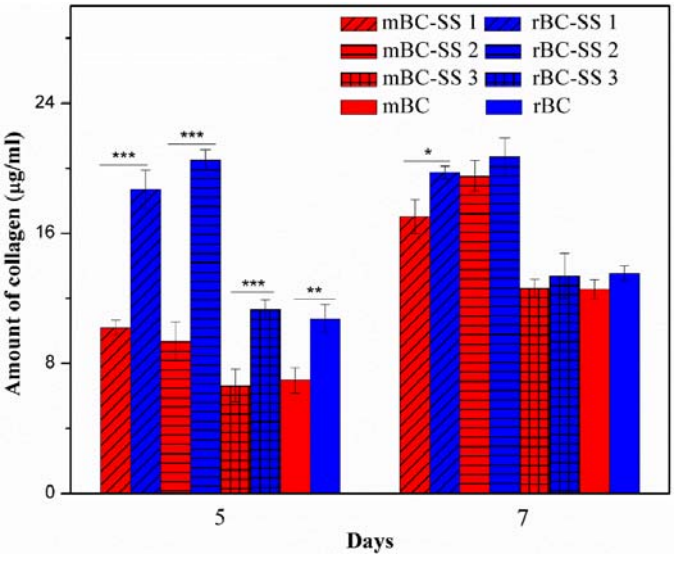

Fig. 7. Soluble collagen production by fibroblasts cultured onto the samples. (***) $P < 0.001$; (**) $P < 0.01$; (*) $P < 0.05$.

At day 5, the level of collagen measured with rBC-SS composites was significantly higher than that with mBC-SS composites, while on the 7th day, the difference was not significant although the trend in collagen production remained unchanged. Moreover, in rBC-SS samples, the collagen production at day 5 remained approximately equal to that at day 7, while with mBC-SS, an increase was observed between these days. This shows high initial collagen synthesis in the presence of rBC-SS due to higher initial cell attachment and higher SS release with these substrates compared with mBC-SS samples where the collagen production is rather progressive. Overall, the high

amount of collagen synthesis at short-term in presence of rBC-SS may be the result of less controlled proliferation of fibroblasts with cell agglutination as observed on confocal images, which would lead to a non-homogeneous deposition of collagen thus resulting in fibrosis. By contrast, the progressive synthesis of collagen in the presence of mBC-SS composites can be explained by a controlled proliferation of fibroblasts by their alignment along the lines of mBC, which would induce progressive and homogeneous deposition of collagen in the direction of the arrangement of the cells.

4 Conclusions

The mBC-SS and rBC-SS composites as wound dressings were compared with regard to their bioactivity as well as the ability to reduce fibrosis and scar formation. mBC and mBC-SS composites exhibit well-aligned and compact fiber networks while these fibers are randomly arranged in rBC and its composites. However, rBC is more porous compared to mBC, which is beneficial for water absorption. The water uptake abilities of the composites varied with SS concentration, but all had good absorptive capacities as required for dressing application so that to support exudates removal. *In vitro* and under physiological conditions, the BC-SS2 composites which appear to be most optimal for dressing applications could release sufficient SS in a short time, which improved the proliferation of fibroblast and epithelial cells as well as collagen synthesis.

On mBC-SS composites, fibroblasts were aligned according to the orientation of the microgrooves while randomly arranged on rBC-SS. As fibroblasts were responsible for the synthesis of collagen, it was anticipated that the deposition of the latter would be carried out according to the alignment of the cells, limiting fibrosis and scar formation. Keratinocytes had similar morphologies on both types of composites, with a tendency to be aligned on mBC-based samples. Overall, mBC-SS composites represent promising biomaterials for wound dressing application to guide fibroblast alignment and proliferation, thus controlling the deposition of collagen and minimizing fibrosis. Further *in vivo* studies would help demonstrate the aligned deposition of collagen, the inherent immunological response and wound healing outcome in order to confirm the ability of mBC-SS as wound dressing.

Acknowledgement

This work was supported by the National Natural Science Foundation of China [grant numbers 21774039, 51973076].

Supporting information

Not applicable

Conflict of interest

There are no conflicts to declare.

References

[1] A. N. Dehkordi, F. M. Babaheydari, M. Chehelgerdi and S. R. Dehkordi, *Stem Cell Res Ther*, 2019, **10**, 111. https://doi:10.1186/s13287-019-1212-2

[2] A. Wells, A. Nuschke and C. C. Yates, *Matrix Biol*, 2016, **49**, 25-36. https://doi:10.1016/j.matbio.2015.08.001

[3] E. Y. X. Loh, N. Mohamad, M. B. Fauzi, M. H. Ng, S. F. Ng and M. C. I. M. Amin, *Sci. Rep*, 2018, **8**, 2875. https://doi:10.1038/s41598-018-21174-7

[4] S. Napavichayanun, R. Yamdech and P. Aramwit, *Int J Polym Mater*, 2018, **67**, 61-67. https://doi:10.1080/00914037.2017.1297943

[5] D. Zmejkoski, D. Spasojevic, I. Orlovska, N. Kozyrovska, M. Sokovic, J. Glamoclija, S. Dmitrovic, B. Matovic, N. Tasic, V. Maksimovic, M. Sosnin and K. Radotic, *Int J Biol Macromol*, 2018, **118**, 494-503. https://doi:10.1016/j.ijbiomac.2018.06.067

[6] Y. Li, S. Qing, J. Zhou and G. Yang, *Carbohydr. Polym*, 2014, **103**, 496-501. https://doi:10.1016/j.carbpol.2013.12.059

[7] X. Wen, Y. Zheng, W. Jian, L. Yue, W. Cai, J. Luan, Z. Wu and K. Wang, *Prog. Nat. Sci*, 2015, **25**, 197-203. https://doi:10.1016/j.pnsc.2015.05.004

[8] M. Fürsatz, M. Skog, P. Sivlér, E. Palm, C. Aronsson, A. Skallberg, G. Greczynski, H. Khalaf, T. Bengtsson and D. Aili, *Biomed Mater*, 2018, **13**, 025014. https://doi:10.1088/1748-605X/aa9486

[9] J. Wu, Y. Zheng, W. Song, J. Luan, X. Wen, Z. Wu, X. Chen, Q. Wang and S. Guo, *Carbohydr. Polym*, 2014, **102**, 762-771. https://doi:10.1016/j.carbpol.2013.10.093

[10] S. Napavichayanun, R. Yamdech and P. Aramwit, *Arch Dermatol Res*, 2016, **308**, 123-132. https://doi:10.1007/s00403-016-1621-3

[11] T. Siritientong, A. Angspatt, J. Ratanavaraporn and P. Aramwit, *Pharm. Res.*, 2014, 31, 104-116. https://doi:10.1007/s11095-013-1136-y

[12] P. Aramwit and A. Sangcakul, *Bioscience, Biosci Biotech, Bioch*, 2007, **71**, 2473-2477. https://doi:10.1271/bbb.70243

[13] P. Aramwit, T. Siritienthong, T. Srichana and J. Ratanavaraporn, *Cells Tissues Organs*, 2013, **197**, 224-238. https://doi:10.1159/000345600

[14] Y.-Y. Jo, D.-W. Kim, J.-Y. Choi and S.-G. Kim, *Sci Rep*,, 2019, **9**, 3448. https://doi:10.1038/s41598-019-40027-5

[15] M. Jang, Park, B., Kweon, H., Jo, Y., and Um, I.,, *Int. J. Indust. Entomol*, 2015, **31**, 1-6. https://doi:10.7852/ijie.2015.31.1.1

[16] L. Lamboni, Y. Li, J. A. Liu and G. Yang, *Biomacromolecules*, 2016, **17**, 3076-3084. https://doi:10.1021/acs.biomac.6b00995

[17] M. Jin, Chen, W. , Li, Z. , Zhang, Y. , Zhang, M. , & Chen, S., *Cellulose*, 2018, **25**, 6705-6717. https://doi:10.1007/s10570-018-2041-7

[18] R. M. Visalakshan, A. A. Cavallaro, M. N. MacGregor, E. P. Lawrence, K. Koynov, J. D. Hayball and K. Vasilev, *Adv Funct Mater*, 2019, **29**, 1807453. https://doi:10.1002/adfm.201807453

[19] Y. Yang, K. Wang, X. Gu and K. W. Leong, *Engineering*, 2017, **3**, 36-54. https://doi:10.1016/J.ENG.2017.01.014

[20] M. C. T. Asuncion, J. C. Goh and S. L. Toh, *Mat Sci Eng. C-Mater*, 2016, **67**, 646-656. https://doi:10.1016/j.msec.2016.05.087

[21] M. Georgiou, S. C. J. Bunting, H. A. Davies, A. J. Loughlin, J. P. Golding and J. B. Phillips, *Biomaterials*, 2013, **34**, 7335-7343. https://doi:10.1016/j.biomaterials.2013.06.025

[22] A. L. Oliveira, L. Sun, H. J. Kim, X. Hu, W. Rice, J. Kluge, R. L. Reis and D. L. Kaplan, *Acta Biomater*, 2012, **8**, 1530-1542. https://doi:10.1016/j.actbio.2011.12.015

[23] G. Lu, Z. Ding, Y. Wei, X. Lu, Q. Lu and D. L. Kaplan, *ACS Appl Mater Interfaces*, 2018, **10**, 44314-44323. https://doi:10.1021/acsami.8b18626

[24] Y. Hu, H. Liu, X. Zhou, H. Pan, X. Wu, N. Abidi, Y. Zhu and J. Wang, *Mat Sci Eng. C-Mater*, 2019, **99**, 333-343. https://doi:10.1016/j.msec.2019.01.116

[25] S. Bottan, F. Robotti, P. Jayathissa, A. Hegglin, N. Bahamonde, J. Heredia-Guerrero, A. Scarpellini, H. Merker, N. Lindenblatt, D. Poulikakos and A. Ferrari, *ACS nano*, 2014, **9**, 206-209. https://doi:10.1021/nn5036125

[26] N. Geisel, J. Clasohm, X. Shi, L. Lamboni, J. Yang, K. Mattern, G. Yang, K. H. Schäfer and M. Saumer, *Small*, 2016, **12**, 5407-5413. https://doi:10.1002/smll.201601679

[27] L. Lamboni, C. Xu, J. Clasohm, J. Yang, M. Saumer, K.-H. Schäfer and G. Yang, *Mater. Sci. Eng. C*, 2019, **102**, 502-510. https://doi:10.1016/j.msec.2019.04.043

[28] Y. Li, S. Wang, R. Huang, Z. Huang, B. Hu, W. Zheng, G. Yang and X. Jiang, *Biomacromolecules*, 2015, **16**, 780-789. https://doi:10.1021/bm501680s

[29] P. R. F. d. S. Moraes, S. Saska, H. Barud, L. R. d. Lima, V. d. C. A. Martins, A. M. d. G. Plepis, S. J. L. Ribeiro and A. M. M. Gaspar, *Mater. Res.*, 2016, **19**, 106-116. https://doi:10.1590/1980-5373-MR-2015-0249

[30] L. K. H. Rocha, L. I. L. Favaro, A. C. Rios, E. C. Silva, W. F. Silva, T. Pasquoto, M. Guilger, R. Lima, J. M. O. Jr and N. Aranha, *Process Biochem*, 2017, **61**, 163-177. https://doi:10.1016/j.procbio.2017.06.019

[31] A. Khalid, R. Khan, M. Ul-Islam, T. Khan and F. Wahid, *Carbohydr. Polym*, 2017, **164**, 214-221. https://doi:10.1016/j.carbpol.2017.01.061

[32] D. Gupta, A. Agrawal and A. Rangi, *Indian J Fibre Text*, 2014, **39**, 364-372.

[33] E. Altun, M. O. Aydogdu, F. Koc, M. Crabbe-Mann, F. Brako, R. Kaur-Matharu, G. Ozen, S. E. Kuruca, U. Edirisinghe and O. Gunduz, *Macromol Mater Eng*, 2018, **303**, 1700607. https://doi:10.1002/mame.201700607

[34] C. M. Nelson and C. S. Chen, *FEBS letters*, 2002, **514**, 238-242. https://doi:10.1016/s0014-5793(02)02370-0

[35] B. O. O. Boni, L. Lamboni, T. Souho, M. Gauthier and G. Yang, *Mater. Horiz.*, 2019, **6**, 1122-1137. https://doi:10.1039/C9MH00291J

[36] F. G. Torres, S. Commeaux and O. P. Troncoso, *J Funct Biomater*, 2012, **3**, 864-878. https://doi:10.3390/jfb3040864

[37] P. Aramwit, S. Kanokpanont, W. De-Eknamkul, K. Kamei and T. Srichana, *J Biomater Sci. Polym Ed*, 2009, **20**, 1295-1306. https://doi:10.1163/156856209x453006